ACCOUNTS
of chemical research

Studies on Metal–Organic Frameworks of Cu(II) with Isophthalate Linkers for Hydrogen Storage

YONG YAN, SIHAI YANG, ALEXANDER J. BLAKE, AND
MARTIN SCHRÖDER*
School of Chemistry, University of Nottingham, Nottingham NG7 2RD, U.K.

RECEIVED ON FEBRUARY 27, 2013

CONSPECTUS

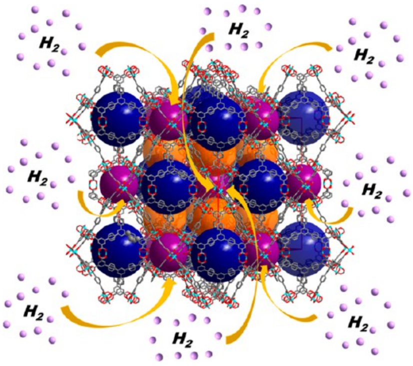

Hydrogen (H_2) is a promising alternative energy carrier because of its environmental benefits, high energy density, and abundance. However, development of a practical storage system to enable the "Hydrogen Economy" remains a huge challenge. Metal–organic frameworks (MOFs) are an important class of crystalline coordination polymers constructed by bridging metal centers with organic linkers. MOFs show promise for H_2 storage owing to their high surface area and tuneable properties.

In this Account, we summarize our research on novel porous materials with enhanced H_2 storage properties and describe frameworks derived from 3,5-substituted dicarboxylates (isophthalates) that serve as versatile molecular building blocks for the construction of a range of interesting coordination polymers with Cu(II) ions.

We synthesized a series of materials by connecting linear tetracarboxylate linkers to $\{Cu(II)_2\}$ paddlewheel moieties. These materials exhibit high structural stability and permanent porosity. Varying the organic linker modulates the pore size, geometry, and functionality to control the overall H_2 adsorption. Our top-performing material in this series has a H_2 storage capacity of 77.8 mg g^{-1} at 77 K, 60 bar. H_2 adsorption at low, medium, and high pressures correlates with the isosteric heat of adsorption, surface area, and pore volume, respectively.

Another series, using tribranched C_3-symmetric hexacarboxylate ligands with Cu(II), gives highly porous (3,24)-connected frameworks incorporating $\{Cu(II)_2\}$ paddlewheels. Increasing the length of the hexacarboxylate struts directly tunes the porosity of the resultant material from micro- to mesoporosity. These materials show exceptionally high H_2 uptakes owing to their high surface area and pore volume. The first member of this family reported adsorbs 111 mg g^{-1} of H_2, or 55.9 g L^{-1}, at 77 K, 77 bar, while at 77 K, 1 bar, the material adsorbs 2.3 wt % H_2. We and others have since achieved enhanced H_2 adsorption in these frameworks using combinations of polyphenyl groups linked by alkynes. The maximum storage achieved for one of the enhanced materials is 164 mg g^{-1} at 77 K, 70 bar, but because of its low density, its volumetric capacity is only 45.7 g L^{-1}.

We attribute the significant adsorption of H_2 at low pressures to the arrangement of the $\{Cu_{24}(isophthalate)_{24}\}$ cuboctahedral cages within the polyhedral structure. Free metal coordination positions are the first binding sites for D_2, and these frameworks have two types of Cu(II) centers, one with its vacant site pointing into the cuboctahedral cage and another pointing externally. D_2 molecules bind first at the former position and then at the external open metal sites.

Design of ligands and complexes is key for enhancing and maximizing H_2 storage, and although current materials operate at 77 K, research continues to explore routes to high capacity H_2 storage materials that can function at higher temperatures.

1. Introduction

Hydrogen (H_2) is a promising energy carrier due to the absence of any carbon emissions at the point of use. H_2 has a high energy density (33.3 kWh/kg) compared with hydrocarbons (12.4–13.9 kWh/kg), but the development of new H_2 storage materials has become one of the major technological barriers and challenges to realizing the "Hydrogen Economy".[1] Solid-state H_2 storage systems based on chemisorption and physisorption have been extensively studied over recent years, but none has satisfied the DOE's 2017 targets for H_2 storage systems: 5.5 wt % in gravimetric terms and 40 g L^{-1} in volumetric capacity of H_2 at an operating temperature of −40 to 60 °C and at pressure below 100 atm.[2] Physisorption of H_2 in porous solids is an attractive option since it can show fast kinetics and favorable thermodynamics in adsorption and release cycles.[3]

10.1021/ar400049h

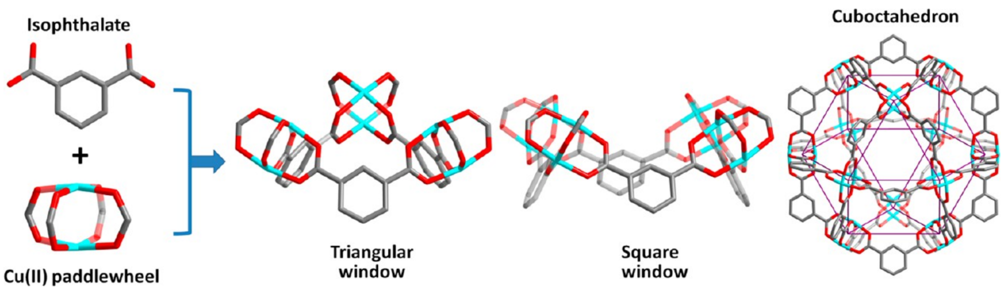

FIGURE 1. Assembly of isophthalate linkers and Cu(II) paddlewheels.

Porous metal–organic frameworks (MOFs) are an important class of crystalline coordination polymer solids constructed from metal centers bridged by organic linkers and are being intensively studied for H_2 storage due to their high internal surface areas and pore volumes.[4] The modular nature of MOFs allows tuning of framework topologies, pore size, and geometry to enhance H_2 adsorption properties.[5] MOFs with very high surface area (>3000 m^2 g^{-1}) show significant H_2 uptake but only at low temperatures (usually 77 K) owing to low isosteric heats of adsorption involved (typically 5–8 kJ mol^{-1}). Strategies to enhance the H_2 binding in these porous hosts include generating frameworks with narrow pores such that the greater overlapping potentials of the pore walls increase the H_2–framework interactions,[6] incorporation of exposed metal sites to afford strong binding sites for H_2,[7] doping with metal ions[8] such as Li^+ and Mg^{2+}, cation exchange to introduce strong electrostatic fields within the cavities,[9,10] and doping of frameworks with metal nanoparticles to increase H_2 uptake via spillover.[4]

In this Account, we describe our research in the synthesis of framework materials derived from isophthalate linkers to paddlewheel $\{Cu_2(OOCR)_4\}$ moieties. We describe synthetic strategies to enhance the H_2 adsorption capacity and binding energies in these porous hosts via the assembly of polyaromatic linear and tri- and tetrabranched isophthalate-containing linkers with varied geometries, and we discuss neutron diffraction studies that have probed preferred D_2 binding sites within these systems.

2. Porous MOFs Containing Isophthalate Linkers with Cu(II) Paddlewheels

A large number of Cu(II) paddlewheel-based MOFs with various topologies showing permanent porosity and stability have been constructed via the self-assembly of aromatic carboxylates and Cu(II) salts.[11,12] Variation of the linkers can efficiently introduce different pore metrics and functionalities. The coordinated solvent molecules on the Cu(II) paddlewheel can be removed via heat treatment *in vacuo* after solvent exchange[5] or by treatment with supercritical CO_2[13] affording materials incorporating exposed Cu(II) sites, which show affinity to guest molecules such as H_2.[4,5] Meta-(3,5)-substituted isophthalate linkers are effective linkers for the assembly of porous frameworks incorporating $[Cu_2(OOCR)_4]$ paddlewheel building units, which act as 4-connected square nodes binding to four independent isophthalate units. Cuboctahedral cages are formed by assembly of 24 isophthalate moieties and 12 $\{Cu(II)_2\}$ paddlewheel units,[14] and this generates a triangular window formed by three isophthalates and three $\{Cu(II)_2\}$ units, and a square window consisting of four isophthalates and four $\{Cu(II)_2\}$ paddlewheels (Figure 1). The 3,5-isophthalate can be functionalized and extended with different organic groups, thus affording carboxylate linkers of differing lengths and substitution patterns.[15]

2.1. Tetracarboxylate Frameworks. A range of rigid aromatic tetracarboxylate struts (Figure 2) has been developed for the construction of porous $\{Cu(II)_2\}$ paddlewheel based MOFs featuring high specific surface areas and H_2 storage capacities.[20−26] In the structures assembled from linkers $(L^1)^{4-}$ to $(L^{14})^{4-}$, the tetracarboxylate struts serve as planar 4-connected nodes when combined with the 4-connected $\{Cu(II)_2\}$ moieties, affording (4, 4)-connected networks with **fof** topology. The **fof**-type network can also be viewed as a Kagomé lattice formed by the triangular and hexagonal windows of $\{Cu(II)_2\}$ paddlewheels pillared by isophthalate linking bridges, and the packing of two types of cages, $[Cu_{12}L_{12}]$ and $[Cu_{24}L_6]$, of the same molecular D_{3d} symmetry generates the tiling of the **fof**-type network (Figure 3). The sizes of the $[Cu_{12}L_{12}]$ and $[Cu_{24}L_6]$ cages are significantly increased by elongation of the organic linkers. However, when the bridge is lengthened beyond a certain point, as in the case of NOTT-104 where the linking bridge between the two isophthalates reaches three phenyl rings, interpenetration of **fof** networks is observed, and this drastically lowers the porosity of the resultant material. When a bulky aromatic moiety is incorporated in the tetracarboxylate ligand backbone as in NOTT-109, the (4,4)-connected

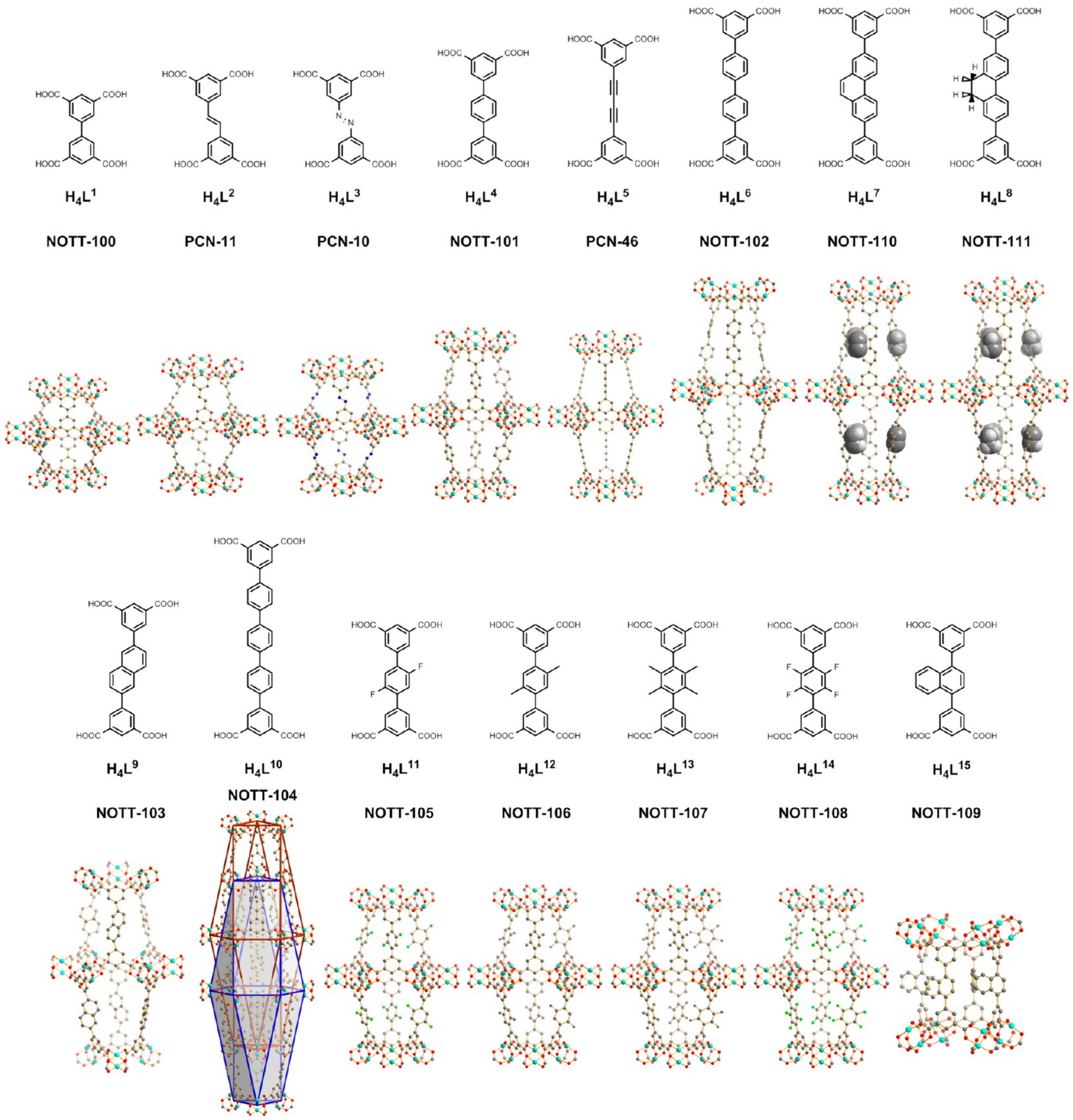

FIGURE 2. Isophthalate tetracarboxylate linkers and their corresponding Cu(II)-based framework materials.

network adopts a different network topology to give an **ssb** net (Figure 4) consisting of only square windows formed by $\{Cu(II)_2\}$ paddlewheels and isophthalate units.

The non-interpenetrating **fof**-type Cu(II) based frameworks show high permanent porosity and BET surface areas in the range 1640 to 2960 $m^2\ g^{-1}$ (Table 1). Due to the nature of physisorbed H_2 in these porous materials, frameworks with high surface area often show high H_2 adsorption capacities. Thus, in the series NOTT-100 to NOTT-102,[16] the pore volume and surface area increase with the increasing length of the ligand backbone, leading to an increase in overall H_2 adsorption capacities at saturation. MOFs with large pores require high pressure to achieve saturation. However, there may be an optimum pore size and pore dimension that optimize H_2 uptake capacities. NOTT-103 incorporates a naphthalene group in the linker and has a pore size intermediate between NOTT-101 and NOTT-102. However, NOTT-103 shows a higher H_2 storage capacity: 65.1 mg g^{-1} at 77 K, 20 bar; 77.8 mg g^{-1} at 60 bar.[17] Low-pressure H_2 adsorption capacity is strongly correlated with

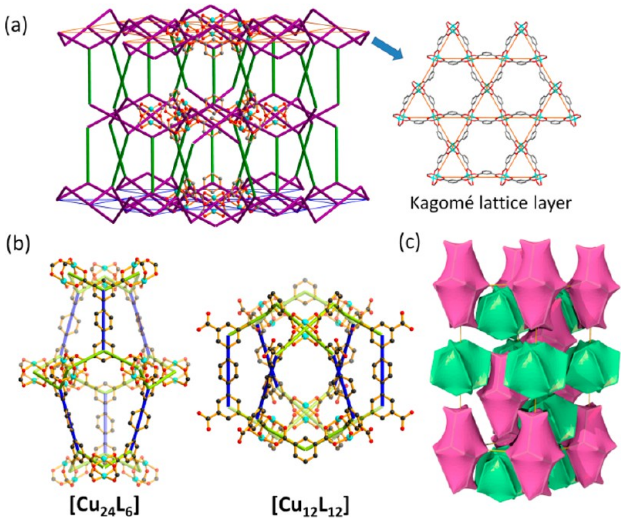

FIGURE 3. Views of (a) the **fof**-type framework viewed as a Kagomé lattice; (b) ellipsoidal [$Cu_{24}L_6$] cage and a spherical [$Cu_{12}L_{12}$] cage; (c) the tiling of these two cages in 3D space to give an **fof**-topology.

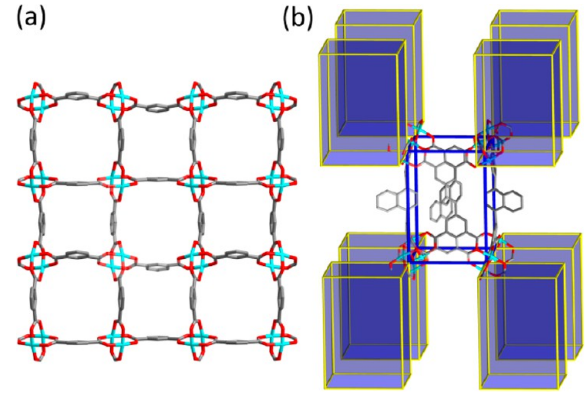

FIGURE 4. Views of (a) the square grid formed by isophthalate units and $\{Cu(II)_2\}$ paddlewheels in NOTT-109; (b) the framework of NOTT-109 with **ssb**-type topology.[17]

the interaction of H_2 with the framework, and the NOTT series of frameworks with accessible open Cu(II) sites shows high H_2 uptakes exceeding 2.2 wt % at 77 K, 1 bar, higher than the H_2 capacities in most other MOFs without exposed metal sites under the same conditions.[17] The role of open metal sites in NOTT-101 in binding H_2 has been confirmed by neutron powder diffraction studies, which also reveal that, in addition to open metal sites, pore functionality and geometry can affect the H_2 affinity. Small pores generate higher H_2 affinity due to the overlap potential from opposite pore walls compared with larger pores.[21] NOTT-100 has channels in the diameter range 8–10 Å and can adsorb 2.59 wt % [wt % = (weight of adsorbed H_2)/(weight of host material)] of H_2 at 77 K, 1 bar, higher than NOTT-101 and NOTT-102 with larger pores. However, NOTT-103 shows a

TABLE 1. Porosity Data and H_2 Sorption Properties of Cu–Tetracarboxylate Frameworks

	complex												
	NOTT-100[16]	PCN-11[19]	PCN-10[19]	NOTT-101[16]	PCN-46[20]	NOTT-102[16]	NOTT-103[17]	NOTT-105[17]	NOTT-106[17]	NOTT-107[17]	NOTT-109[17]	NOTT-110[18]	NOTT-111[18]
BET[a] (m^2 g^{-1})	1640	1779	1407	2316	2500	2942	2929	2387	1855	1822	1718	2960	2930
pore volume[a] (cm^3 g^{-1})	0.680	0.91	0.67	0.886	1.012	1.138	1.142	0.898	0.798	0.767	0.705	1.22	1.19
crystal density (g cm^{-3})	0.927	0.749	0.767	0.650	0.619	0.587	0.643	0.730	0.720	0.756	0.790	0.614	0.617
pore diameter[b] (Å)	6.5			7.3	6.8[d]	8.3	8.0	7.3	7.3	7.0	6.9	8.0	8.0
total H_2 uptake[c] (wt %) at 1 bar/77 K	2.59	2.55	2.34	2.52	1.95	2.24	2.63	2.52	2.29	2.26	2.33	2.64	2.56
total H_2 uptake[c] (mg g^{-1}) at 20 bar/60 bar/77 K	40.2/–	59.7 (45 bar)	52.3 (45 bar)	60.6/66.0	–/71.6	60.7/72.0	65.1/77.8	54.0/–	45.0/–	44.6/–	41.5/–	65.9/76.2	64.8/73.6
volumetric total H_2 uptake at 77 K (g L^{-1})	37.3 (20 bar)	44.7 (45 bar)	39.2 (45 bar)	42.9 (60 bar)	44.32 (60 bar)	42.3 (60 bar)	50.0 (60 bar)	39.4 (20 bar)	32.4 (20 bar)	33.7 (20 bar)	32.8 (20 bar)	46.8 (55 bar)	45.4 (48 bar)

[a] Derived from N_2 isotherms. [b] Pore diameters estimated from Dubinin–Astakhov analysis. [c] H_2 adsorption data at 1 and 20 bar were obtained by gravimetric methods, and data at 60 bar were obtained by volumetric methods; wt % = 100[(weight of adsorbed H_2)/(weight of host)]. [d] The pore diameter of PCN-46 was calculated using the Horvath–Kawazoe model.

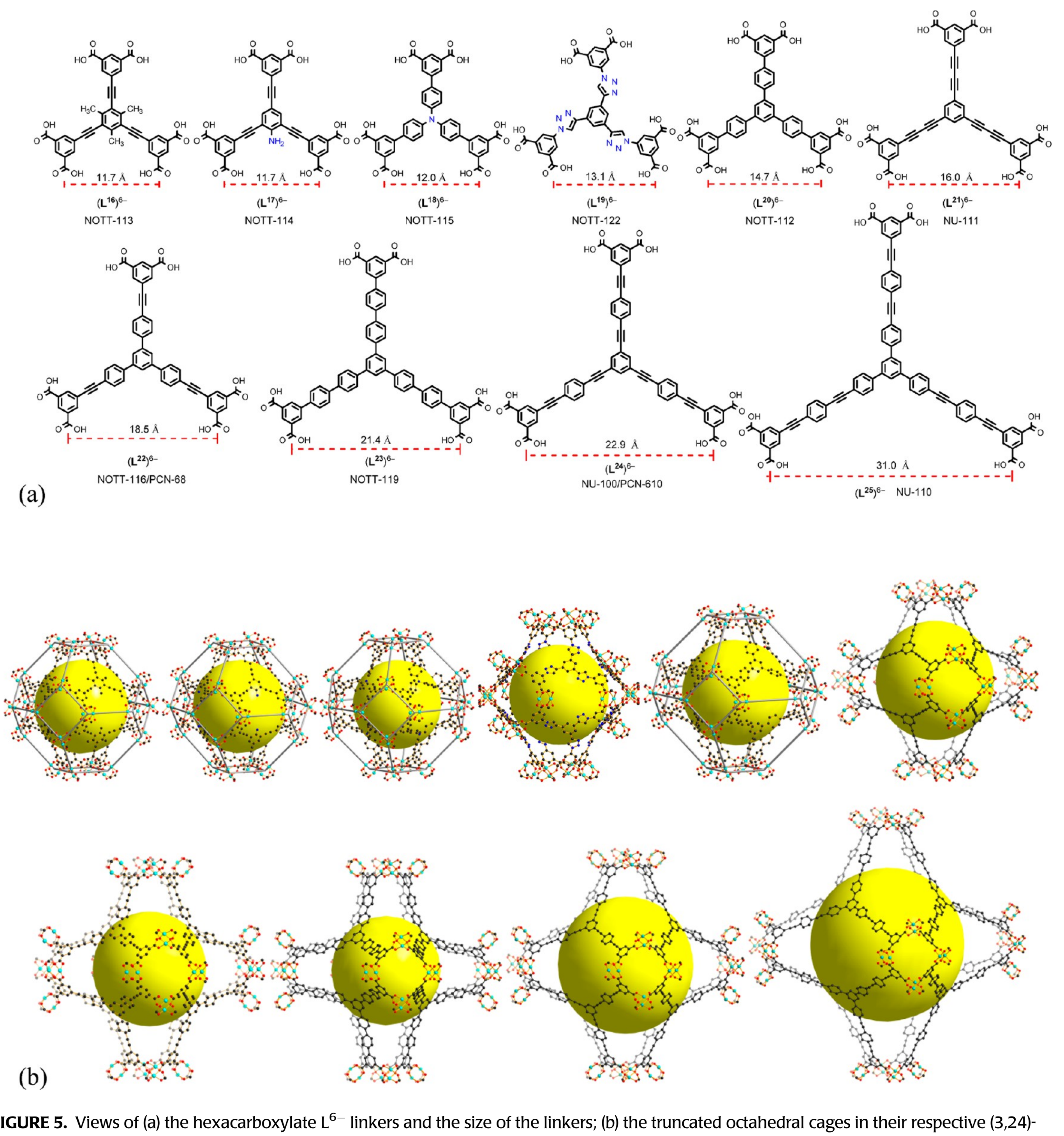

FIGURE 5. Views of (a) the hexacarboxylate L^{6-} linkers and the size of the linkers; (b) the truncated octahedral cages in their respective (3,24)-connected frameworks.

higher H_2 uptake of 2.63 wt % at 77 K, 1 bar, confirming that the naphthyl moiety creates an optimized pocket around the triangular $\{(Cu_2)_3(\text{isophthalate})_3\}$ window, thus giving rise to enhanced H_2 binding interactions.[17]

Incorporation of functional moieties such as methyl and fluorine groups on the framework walls can enhance the enthalpy of adsorption. Functionalized NOTT-105, NOTT-106, and NOTT-107 show significantly higher heat of adsorption for H_2 than NOTT-101. NOTT-107 with four methyl substituents in the central phenyl ring of the linker shows the highest heat of adsorption of 6.70 kJ mol^{-1} at zero coverage in this NOTT series of compounds.[17] However, the reduced pore volume and surface area caused by bulky organic groups lower the overall H_2 adsorption capacity. The introduction of phenanthrene and 9,10-hydrophenanthrene groups into the linking bridges of the

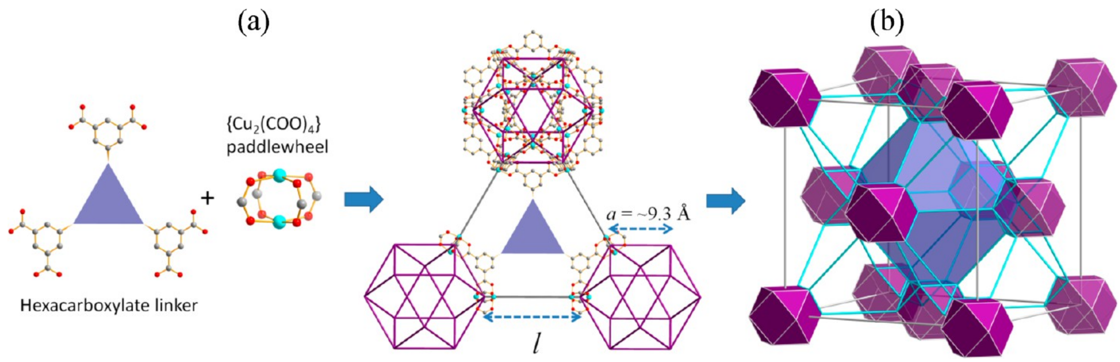

FIGURE 6. Views of (a) the construction of **ubt**-type networks using hexacarboxylate linkers and $\{Cu(II)_2\}$ paddlewheels; (b) the face-centered cubic packing of cuboctahedra in (3,24)-connected networks.

tetracarboxylates has proven to be a successful strategy[18] to enhance the H_2 uptake at low pressures without reducing the total uptake at high pressure. Introducing organic moieties with large molecular areas into the cavity walls has the advantage of generating frameworks with large pore volume and high surface area. Indeed, NOTT-110 and NOTT-111 show high total H_2 uptakes of 76.2 and 73.6 mg g^{-1} at 55 and 48 bar, 77 K, respectively, higher than their structural analogue NOTT-102 (72.0 mg g^{-1} at 60 bar, 77 K). Both of these frameworks also have high H_2 adsorption of 2.64 and 2.56 wt % at 1 bar, 77 K, among the highest for MOFs containing open metal sites, suggesting that the extramolecular surface area introduced by phenanthrene and hydrophenanthrene groups does indeed promote H_2−framework interactions. NOTT-111 shows a higher initial heat of H_2 adsorption than NOTT-110 and NOTT-102, suggesting that the bulkier and non-conjugated 9,10-hydrophenanthrene substituent provides stronger binding sites for H_2 molecules.[18]

2.2. Hexacarboxylate Frameworks. Increasing the length of the organic struts in **fof**-type networks is an effective methodology for generating structures with large pores and high surface area and giving enhanced H_2 adsorption capacities. However, when the ligand bridges are lengthened beyond a certain point, this strategy appears to fail due to the onset of interpenetration, which reduces the available pore volume and appears to also lower structural stability.[17] We argued that a more highly connected network topology might be less likely to form interpenetrated structures. Also, when fused within a network structure, highly connected metal−organic polyhedra may better maintain their intrinsic porosity on tessellation in 3D space.[22] Maximizing the surface area, incorporating open metal sites, and optimizing the pore size and geometry are all essential routes to achieve high H_2 adsorption capacity in framework materials. Taking these strategies into consideration, we designed a series of elongated rigid hexacarboxylate ligands (Figure 5) for the construction of frameworks with $\{Cu(II)_2\}$ paddlewheel units.[23−27]

In all of these isostructural frameworks, the hexacarboxylate linker comprises three coplanar isophthalate units connected through a rigid triangular central core carrying varied chemical composition and functionality. In the MOF products, 24 isophthalate moieties from 24 different L^{6-} units self-assemble into a cuboctahedral cage containing 12 $\{Cu(II)_2\}$ paddlewheels. The central organic core serves as a 3-connected node to link three cuboctahedra, thus forming the (3,24)-connected network with **ubt** topology,[28−34] and each hexacarboxylate L^{6-} unit connects with six $\{Cu(II)_2\}$ paddlewheels to generate a hexagonal face. The **ubt** network can be viewed as the packing of three types of metal−organic polyhedra: a cuboctahedron (cage A), a truncated tetrahedron (cage B) comprising four hexagonal faces and four triangular $\{(Cu_2)_3(\text{isophthalate})_3\}$ windows, and a truncated octahedron (cage C), which is formed by eight hexagonal faces and six square $\{(Cu_2)_4(\text{isophthalate})_4\}$ windows. The cages in the **ubt**-type network are in a ratio 1:2:1 for cage A/cage B/cage C, respectively (Figure 6). The cuboctahedron is comprised of the two types of windows, which share edges of 9.3 Å, and encompasses an inner spherical cavity of ca. 13 Å in diameter. The sizes of cages B and C are proportional to the size of the hexacarboxylate linker (defined by the distance *l* between the centers of two adjacent carboxylates from two separate isophthalates in branched arms of the L^{6-} unit). The (3,24)-connected frameworks of NOTT-112 to NOTT-116[23−25] (NOTT-116 is also known as PCN-68[31]) and NOTT-119[26] incorporate face-centered cubic (fcc) packing of the cuboctahedra, generating nanosized cavities (cage B and C), which are interconnected through the smallest cuboctahedral cages as nodes (Figure 6). This highly connected **ubt** network has the advantage of avoiding network interpenetration. Despite the use of the exceptionally large organic linker, the framework of NOTT-119 is noninterpenetrating and consists of mesocavities of cage B and C with inner sphere diameters of ca. 2.41 and 2.50 nm, respectively.[26]

All the **ubt**-type frameworks show high pore volumes and BET surface areas (Table 2) and significant total H_2 storage capacities at high pressures (Figure 7). NOTT-112, the first system of this type reported,[23] exhibits exceptionally high saturated excess H_2 uptake of 76.1 mg g^{-1} (35 bar, 77 K) and total uptake of 111.1 mg g^{-1} (77 bar, 77 K), and these values are among the highest for highly porous MOFs synthesized to date (Table 2). Increasing the length of the linker in NOTT-112 (BET surface area 3800 m^2 g^{-1}) generates networks with larger cavities and increased BET surface area but lowers the overall excess H_2 uptakes, as in NOTT-116 (68.4 mg g^{-1}, BET 4664 m^2 g^{-1})[32] and NOTT-119 (59.0 mg g^{-1}, BET 4118 m^2 g^{-1}),[26] further indicating that there is an optimum pore size and geometry in these **ubt** frameworks for maximizing the excess H_2 uptake. The pore volume is an important factor for enhancing the total H_2 uptakes of porous frameworks, as larger pore volume materials can hold more H_2 at high pressures. Although NOTT-119 has a lower maximum excess H_2 uptake than NOTT-116, by possessing a larger pore volume of 2.32 cm^3 g^{-1}, it shows nearly the same total H_2 uptake (101.0 mg g^{-1} at 77 K, 60 bar) as NOTT-116 (101.3 mg g^{-1} at 77 K, 50 bar).[24,26] Increasing the length of the hexacarboxylate linkers by using triple-bond spacers can increase the molecule-accessible gravimetric surface areas in these polyhedral structures. Thus, NU-111 and NU-100, which are constructed from linkers incorporating alkyne groups, show especially high BET surface areas of 5000 and 6143 m^2 g^{-1}, respectively.[32,33] NU-111 exhibits a lower maximum excess H_2 uptake of 69 mg g^{-1} at 32 bar, 77 K, compared with NOTT-112, while NU-100 achieves the highest saturated gravimetric capacity (99.5 mg g^{-1}) of all the synthesized **ubt**-type MOFs. Further expanding the hexacarboxylate units leads to a framework NU-110 showing ultrahigh porosity and a record-high surface area of 7140 m^2 g^{-1}.[34]

The volumetric H_2 capacity is a critical criterion for practical transportation applications, and of course, the density of materials plays an important role in defining this capacity. Increasing the length of the hexacarboxylate spacers in the above **ubt** frameworks generates materials with enhanced porosity in terms of pore volume. However, the crystal density drops dramatically when large organic spacers are employed. Thus, although NU-100 has ultrahigh porosity, it shows a total volumetric H_2 uptake of only 45.7 g L^{-1} at

TABLE 2. Porosity Parameters for Cu−Hexacarboxylate Frameworks and Their H_2 Sorption Properties

	material									
	NOTT-113[25]	NOTT-114[25]	NOTT-115[25]	NOTT-122[27]	NOTT-112[23]	NU-111[33]	NOTT-116[24]	NOTT-119[26]	NU-100[32]	NU-110[34]
linker size, *l* (Å)	11.7	11.7	12.0	13.1	14.7	16.0	18.5	21.4	22.9	31.0
unit cell parameters[a] (Å)	$a = 42.712(5)$	$a = 42.710(5)$	$a = 43.127(5)$	$a = 30.926(5)$ $c = 45.103(7)$	$a = 47.005(3)$	$a = 48.893(2)$	$a = 51.670(6)$	$a = 56.296(7)$	$a = 59.872(2)$	$a = 68.706(10)$
crystal density (g cm^{-3})	0.592	0.574	0.611	0.589	0.503	0.408	0.407	0.361	0.279	0.222
cage A size (Å)	13.0	13.0	13.0	13.0	13.0	13.0	13.0	13.0	13.0	13.0
cage B size (Å)	13	13	11	12.2	13.9	17	16	24.1	15.4	21.2
cage C size (Å)	20	20	18	19.3	20	23	24	25	27.4	31.5
BET surface area (m^2 g^{-1})	2970	3424	3394	3286	3800	5000	4664	4118	6143	7140
pore volume (cm^3 g^{-1})	1.25	1.36	1.38	1.41	1.62	2.38	2.17	2.32	2.82	4.4
H_2 uptake (wt %) at 1 bar, 77 K	2.39	2.28	2.42	2.61	2.3	2.1	1.9	1.44	1.8	
maximum excess H_2 uptake (mg g^{-1})	53.7	52.9	59.3		76.1	69	68.4	59.0	99.5	
total H_2 uptake (mg g^{-1})	71.7 (60 bar)	72.4 (60 bar)	80.7 (60 bar)	70.0 (20 bar)	111.1 (77 bar)	135 (110 bar)	101.3 (50 bar)	101.0 (60 bar)	164 (70 bar)	
total volumetric H_2 uptake (g L^{-1})	42.5 (60 bar)	42.6 (60 bar)	49.3 (60 bar)	41.2 (20 bar)	55.9 (77 bar)	55.1 (110 bar)	41.2 (50 bar)	36.5 (60 bar)	45.7 (70 bar)	
H_2 enthalpy, Q_{st} (kJ mol^{-1})	5.9	5.3	5.8	6.0	5.6	5.6	6.7	7.3	6.1	

[a] The Cu−hexacarboxylate frameworks crystallize in the cubic space group $Fm\bar{3}m$ except for NOTT-122, which adopts the lower-symmetry tetragonal space group $I4/m$.

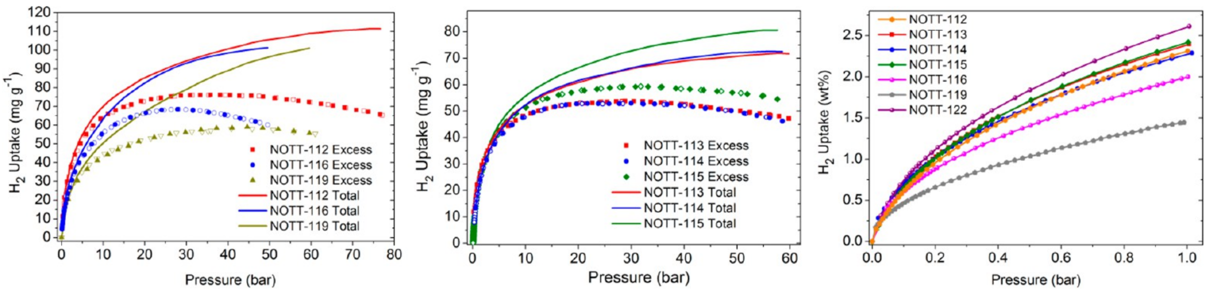

FIGURE 7. H_2 sorption isotherms at 77 K for Cu−hexacarboxylate frameworks.

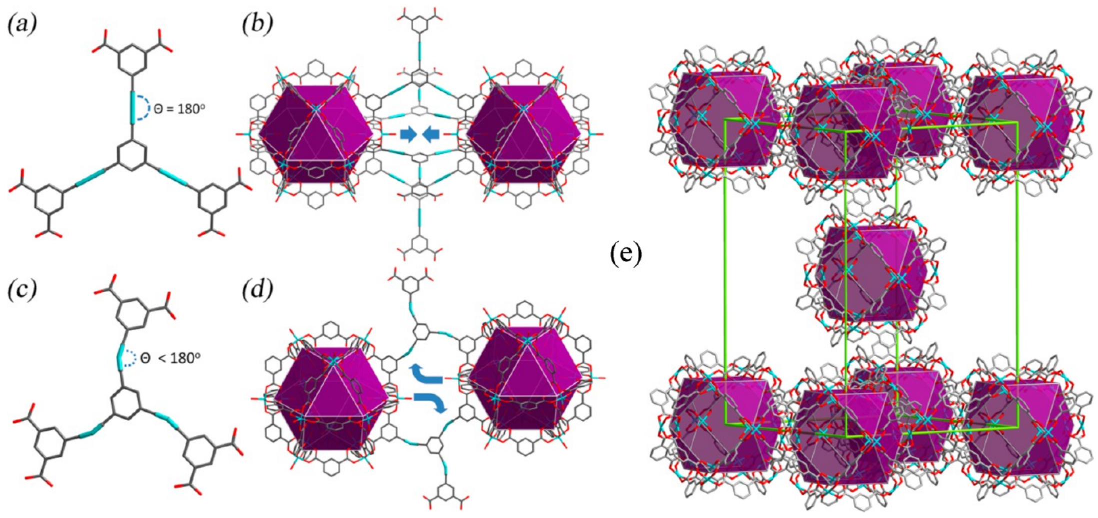

FIGURE 8. Views of C_3-symmetric hexacarboxylate linkers and the resultant Cu−carboxylate network structures. (a) Coplanar linearly connected isophthalates. (b) Two closest cuboctahedra in the **ubt**-type network aligned on the same axis showing steric hindrance (blue arrows) from the two axial water molecules. (c) Coplanar angularly connected isophthalate units showing a lowered symmetry. (d) Enhanced close-packing of the cuboctahedra compared with the fcc-**ubt** network. (e) The body-centered tetragonal packing of $\{Cu_{24}\}$ cuboctahedra in NOTT-122. Reproduced with permission of The Royal Society of Chemistry from ref 27.

70 bar, 77 K,[32,33] lower than the shorter-linked analogues NOTT-115 (49.3 g L^{-1}, 60 bar, 77 K)[25] and medium-sized NOTT-112 (55.9 g L^{-1} at 77 bar, 77 K)[24] (Table 2).

Modulating the cage structures in **ubt**-type networks can effectively tune the H_2 adsorption properties. In NOTT-113, NOTT-114, and NOTT-115, the central core of the hexacarboxylate linkage is decorated by trisalkynylbenzene, triethynylaniline, and triphenylamine, respectively, to afford frameworks containing cages of similar dimensions.[25] NOTT-113 and NOTT-114 exhibit high total H_2 adsorption capacities of 71.7 and 72.4 mg g^{-1} H_2, respectively, at 77 K, 60 bar, while NOTT-115 achieves 80.7 mg g^{-1} total H_2 adsorption at 77 K, 60 bar. Thus, variations of linker length and its functionalization lead to modulation of the uptake capacities and the adsorption enthalpies for this series of materials (Table 2). Incorporation of more aromatic rings (as in NOTT-119) can be used as a strategy to increase H_2−framework interactions.[26]

These Cu(II)-based frameworks show high H_2 uptakes at 1 bar, 77 K, due to the presence of $\{Cu_{24}(\text{isophthalate})_{24}\}$ cuboctahedral cages. Compared with mesoporous NOTT-116 and NOTT-119, NOTT-112−NOTT-115 incorporate shorter hexacarboxylate linkers, and thus the cuboctahedral cages are more closely packed in the latter four frameworks, leading to higher H_2 uptakes (all exceeding 2.2 wt %) at 1 bar. This suggests that design of the hexacarboxylate linker in **ubt** networks can be used to control the separation between these cuboctahedral cages to enhance H_2 adsorption at low pressures. However, there is a limit to the length and size of linkers that can be applied in this (3,24)-connected net to form the fcc-packing of the cuboctahedra, because this type of close packing will be inhibited if there is steric hindrance and repulsion between the two closest axial ligands in the Cu(II) paddlewheel in the two closest cuboctahedra (Figure 8).[27] Thus, modifying the shape of the hexacarboxylate linker by introducing an angular component to

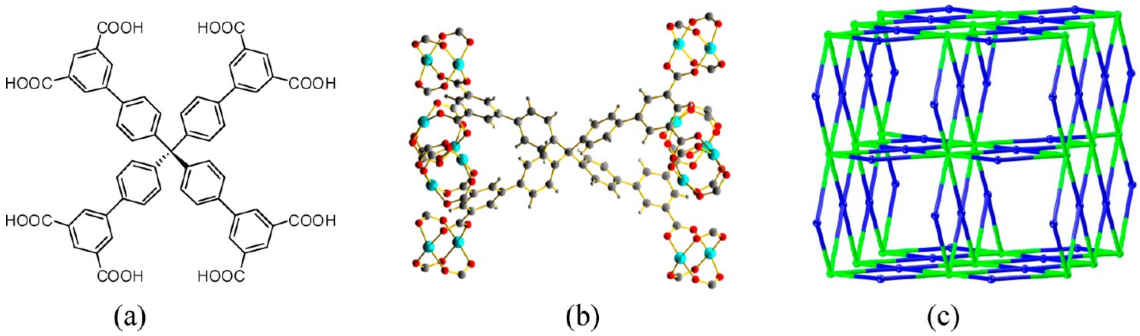

FIGURE 9. Views of (a) the octacarboxylate linker; (b) connectivity of the ligand to eight {Cu(II)$_2$} paddlewheels; and (c) the 4,8-connected **scu**-type network for NOTT-140 (organic linker node: green; {Cu(II)$_2$} paddlewheel node: blue). Reproduced with permission of The Royal Society of Chemistry from ref 35.

the three coplanar isophthalate arms emanating from the C_3-symmetric central core, results in a different type of tight packing of the cuboctahedra as observed in NOTT-122.[27] NOTT-122 shows body-centered tetragonal (bct)-packing of cuboctahedra and the highest H_2 adsorption capacity of 2.61 wt % at 77 K, 1 bar, among all the (3,24)-connected frameworks. The combined effects of the closed bct-packing of the cuboctahedra with exposed Cu(II) sites are both responsible for the high H_2 adsorption capacity in NOTT-122.

2.3. Octacarboxylate Frameworks. Four isophthalates can be linked at the 1-position to a tetratopic organic unit to form an octacarboxylate linker. We have thus combined[35] an aromatic-rich, tetrahedrally branched octacarboxylate strut (H_8L, Figure 9) with {Cu(II)$_2$} paddlewheel building blocks to construct the robust and porous framework NOTT-140, which is a 4,8-connected network of rare **scu**[36] topology. The framework structure of NOTT-140 can be viewed as square grid layers of {(Cu$_2$)$_4$(isophthalate)$_4$} units pillared by the tetratopic organic moieties to generate large one-dimensional channels of 13 × 14 Å^2. Desolvated NOTT-140 shows a high total H_2 uptake of 60.0 mg g^{-1} at 20 bar, 77 K. Due to the open Cu(II) sites and richness of aromatic rings exposed in the pore channels, NOTT-140 adsorbs 2.5 wt % of H_2 at 1 bar, 77 K, comparable to the Cu−tetracarboxylate and Cu−hexacarboxylate frameworks. However, NOTT-140 shows relatively low heat of H_2 adsorption of 4.15 kJ mol^{-1} at zero surface coverage compared with other (3,24)-connected Cu(II)-based frameworks with average adsorption enthalpies of 5.3−7.3 kJ mol^{-1}. This is probably due to the different alignment of vacant Cu(II) sites within the porous structure in NOTT-140 compared with that in the polyhedral frameworks containing the cuboctahedral {Cu$_{24}$(isophthalate)$_{24}$} cages.

3. Neutron Powder Diffraction Studies

A detailed understanding of the H_2 adsorption sites within framework materials is vital for establishing structure−performance correlations and developing materials with enhanced properties. We employed neutron powder diffraction (NPD) to elucidate the site-specific interactions of H_2 within frameworks. NPD data were collected for NOTT-101 at different D_2 loadings, and Rietveld refinement revealed three different hydrogen binding sites.[17] The exposed Cu(II) sites are the first, strongest binding site with a Cu···D_2-(centroid) distance of 2.50(3) Å: this is slightly longer than that observed in HKUST-1[37] (2.40 Å) but is clearly not of the "Kubas" type σ-bond binding. Two other adsorption sites were identified at higher loadings, both coinciding with a 3-fold symmetry axis: one is located in the middle of the triangular {(Cu$_2$)$_3$(isophthalate)$_3$} window, while the other is in the cusp of three phenyl rings (sites II and III, Figure 10). The distances between pairs of sites (site I···site II 3.8 Å, site III···site II 3.8 Å, site I···site III 7.04 Å) are physically reasonable and consistent with the minimum distance allowed between two D_2 molecules (3.4 Å in solid D_2). At 1.82 D_2/Cu loading, the analysis of the occupancies of D_2 at

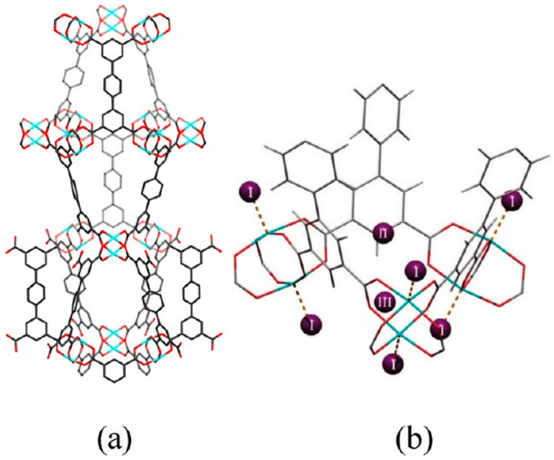

FIGURE 10. Views of (a) structure of NOTT-101 and (b) the three identified D_2 adsorption sites in NOTT-101 by neutron powder diffraction. Reproduced with permission from ref 17. Copyright 2009 American Chemical Society.

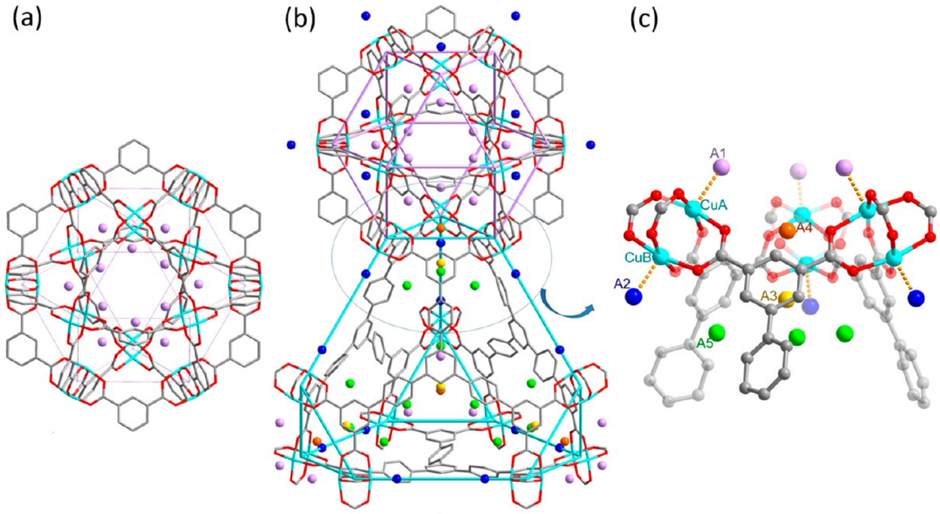

FIGURE 11. Views of D_2 positions in the desolvated framework NOTT-112. (a) D_2 positions in the cuboctahedral cage at a loading of 0.5 D_2/Cu; (b) D_2 positions in cage A and cage B at a loading of 2.0 D_2/Cu; (c) view of five D_2 positions (A1, A2, A3, A4, and A5) at a loading of 2.0 D_2/Cu (gray, carbon; red, oxygen; turquoise, copper). The D_2 positions are represented by colored spheres: A1, lavender; A2, blue; A3, yellow; A4, orange; A5, green. Reproduced with permission from ref 24. Copyright 2010 American Chemical Society.

different sites suggests that D_2 occupies both sites II and III before site I is fully saturated, indicating that the $Cu\cdots D_2$ binding energy for site I is not significantly higher than those for sites II and III.

NPD studies on gas-loaded NOTT-112 revealed that there are differences between the $Cu\cdots H_2$ interactions at the two Cu(II) sites in the same paddlewheel unit.[24] The first and most strongly bound site (site A1, Figure 11) was found at the exposed Cu(II) ions, CuA sited within the cuboctahedral cage, and exhibits a short D_2(centroid)$\cdots$CuA distance of 2.23(1) Å, indicating significant interaction between CuA and D_2. The other Cu(II) ion in the same $\{Cu(II)_2\}$ paddlewheel, CuB, is the second site of binding (A2) with a longer $D_2\cdots$CuB distance of 2.41(1) Å. At low coverage, these two sites are clearly distinguished by their D_2 adsorption behavior, with 85% of the D_2 from the first dosing coordinating to CuA centers, indicating that the two Cu(II) sites exhibit different environments for D_2 binding. The enhanced adsorption of D_2 by CuA is probably due to its being within the cuboctahedral cage, while CuB lies outside the cage. NPD studies on HKUST-1 and NOTT-101, in which all the Cu(II) centers are chemically equivalent, showed no differentiation between the Cu(II) sites for D_2 adsorption. Thus, we provide for the first time direct structural evidence demonstrating that a specific geometrical arrangement of exposed Cu(II) sites, in this case within the $\{Cu_{24}(\text{isophthalate})_{24}\}$ cuboctahedral cage, strengthens the interactions between D_2 molecules and open metal sites. The initial occupation of the three sites A3, A4, and A5 is only observed at higher loading. Sites A3 and A4 are located on the same 3-fold axis of the triangular window with the former being in the cusp of three isophthalate phenyl rings and the latter being on the other side of the window inside the cuboctahedral cage. Site A5 is located within the truncated tetrahedral cage B around the 3-fold axis of the triangular window.

4. Conclusions and Outlook

In this Account, we have described our recent work on the rational design of MOF materials for applications in H_2 storage. These frameworks are derived from organic struts incorporating isophthalate units that provide a diversity of secondary building units for the construction of novel structures with $\{Cu(II)_2\}$ paddlewheels. Variation of the organic moieties that connect with isophthalate units via the 1-position generates a series of tetra-, hexa-, and octacarboxylate aromatic rigid linkers, affording frameworks by the assembly with $\{Cu(II)_2\}$ paddlewheels with versatile pore geometries and functionalities. Polyhedral **ubt**-type frameworks incorporating hierarchically sized cages assembled from hexacarboxylate linkers have higher surface areas and pore volumes than those derived from tetracarboxylates or octacarboxylates and show high H_2 storage capacities. These Cu(II)-based materials show relatively low isosteric heats of adsorption for H_2, typically 5−8 kJ mol^{-1}, despite the incorporation of open Cu(II) sites, which show only slightly higher adsorption energy than other binding sites. Currently, we are exploring further routes to the preparation of porous MOFs, which not only show very high surface areas and pore volumes but also possess high isosteric heats of adsorption for H_2, with the aim of raising the operating temperatures of these materials.

We thank the EPSRC and the University of Nottingham for support. S.Y. thanks that Leverhulme Trust for an Early Career Research Fellowship, and M.S. thanks the ERC for an Advanced Grant.

BIOGRAPHICAL INFORMATION

Yong Yan was born in 1984 in Hubei, China. He obtained his B.Sc. in Chemistry from Lanzhou University, China (2006) and Ph.D. in Chemistry under the supervision of Professor Martin Schröder at the University of Nottingham (2011). His research focuses on novel porous metal–organic materials for clean and renewable energy applications.

Sihai Yang was born in Tianjin, China, in 1984. He received his B.Sc. in Chemistry from Peking University (2007) and Ph.D. in Chemistry under the supervision of Professor M. Schröder at University of Nottingham (2011). He has been awarded the Dorothy Hodgkin Fellowship (2007), an EPSRC PhD Plus Fellowship (2010), and the Leverhulme Trust Early Career Fellowship (2011). He won the Diamond Light Source Young Investigator Award in 2011. His research interests focus on the selective carbon capture and hydrocarbon separations in functional porous materials.

Alexander J. Blake is Professor and Director of Chemical Crystallography at the University of Nottingham. He served as Vice-President of the British Crystallographic Association (2007–2010) and in 2012 was appointed Adjunct Professor at RMIT University, Melbourne, Australia. He is Chair of the European Crystallographic Meeting (ECM28) which took place at the University of Warwick, UK, in August 2013. His research interests include structure determination, supramolecular structure, and high pressure crystallography.

Martin Schröder is Professor and Head of Inorganic Chemistry and Executive Dean of the Faculty of Science at the University of Nottingham. His research interests lie in the area of coordination and supramolecular chemistry with specific focus on energy applications and clean technologies.

FOOTNOTES

*E-mail: M.Schroder@nottingham.ac.uk.
The authors declare no competing financial interest.

REFERENCES

1 Schlapbach, L.; Züttel, A. Hydrogen-Storage Materials for Mobile Applications. *Nature* **2001**, *414*, 353–358.

2 http://www.eere.energy.gov/hydrogenandfuelcells/mypp/. Department of Energy, Office of Energy Efficiency and Renewable Energy Hydrogen, Fuel Cells and Infrastructure Technologies Program Multi-Year Research, Development and Demonstration Plan.

3 Eberle, U.; Felderhoff, M.; Schüth, F. Chemical and Physical Solutions for Hydrogen Storage. *Angew. Chem., Int. Ed.* **2009**, *48*, 2–25.

4 Suh, M. P.; Park, H. J.; Prasad, T. K.; Lim, D.-W. Hydrogen Storage in Metal-Organic Frameworks. *Chem. Rev.* **2012**, *112*, 782–835.

5 Lin, X.; Champness, N. R.; Schröder, M. Hydrogen, Methane and Carbon Dioxide Adsorption in Metal-Organic Framework Materials. *Top. Curr. Chem.* **2010**, *293*, 35–76.

6 Chen, B.; Zhao, X.; Putkham, A.; Hong, K.; Lobkovsky, E. B.; Hurtado, E. J.; Fletcher, A. J.; Thomas, K. M. Surface Interactions and Quantum Kinetic Molecular Sieving for H_2 and D_2 Adsorption on a Mixed Metal-Organic Framework Material. *J. Am. Chem. Soc.* **2008**, *130*, 6411–6423.

7 Dincă, M.; Long, J. R. Hydrogen Storage in Microporous Metal–Organic Frameworks with Exposed Metal Sites. *Angew. Chem., Int. Ed.* **2008**, *47*, 6766–6779.

8 Mulfort, K. L.; Farha, O. K.; Stern, C. L.; Sarjeant, A. A.; Hupp, J. T. Post-Synthesis Alkoxide Formation within Metal-Organic Framework Materials: A Strategy for Incorporating Highly Coordinatively Unsaturated Metal Ions. *J. Am. Chem. Soc.* **2009**, *131*, 3866–3868.

9 Yang, S.; Lin, X.; Blake, A. J.; Walker, G.; Hubberstey, P.; Champness, N. R.; Schröder, M. Cation-induced Kinetic Trapping and Enhanced Hydrogen Adsorption in a Modulated Anionic Metal–Organic Framework. *Nat. Chem.* **2009**, *1*, 487–493.

10 Yang, S.; Martin, G. S. B.; Titman, J. J.; Blake, A. J.; Allan, D. R.; Champness, N. R.; Schröder, M. Pore with Gate: Enhancement of the Isosteric Heat of Adsorption of Dihydrogen via Postsynthetic Cation Exchange in Metal-Organic Frameworks. *Inorg. Chem.* **2011**, *50*, 9374–9384.

11 Perry, J. J., IV; Perman, J. A.; Zaworotko, M. J. Design and synthesis of metal–organic frameworks using metal–organic polyhedra as supermolecular building blocks. *Chem. Soc. Rev.* **2009**, *38*, 1400–1417.

12 Zhao, D.; Timmons, D. J.; Yuan, D.; Zhou, H.-C. Tuning the Topology and Functionality of Metal-Organic Frameworks by Ligand Design. *Acc. Chem. Res.* **2011**, *44*, 123–133.

13 Farha, O. K.; Hupp, J. T. Rational Design, Synthesis, Purification, and Activation of Metal–Organic Framework Materials. *Acc. Chem. Res.* **2010**, *43*, 1166–1175.

14 Moulton, B.; Lu, J.; Mondal, A.; Zaworotko, M. J. Nanoballs: Nanoscale Faceted Polyhedra with Large Windows and Cavities. *Chem. Commun.* **2001**, 863–864.

15 Perry, J. J., IV; Kravtsov, V. Ch.; McManus, G. J.; Zaworotko, M. J. Bottom up Synthesis That Does Not Start at the Bottom: Quadruple Covalent Cross-Linking of Nanoscale Faceted Polyhedra. *J. Am. Chem. Soc.* **2007**, *129*, 10076–10077.

16 Lin, X.; Jia, J.; Zhao, X. B.; Thomas, K. M.; Blake, A. J.; Champness, N. R.; Hubberstey, P.; Schröder, M. High H_2 Adsorption by Coordination-Framework Materials. *Angew. Chem., Int. Ed.* **2006**, *45*, 7358–7364.

17 Lin, X.; Telepeni, I.; Blake, A. J.; Dailly, A.; Brown, C. M.; Simmons, J. M.; Zoppi, M.; Walker, G. S.; Thomas, K. T.; Mays, T. J.; Hubberstey, P.; Champness, N. R.; Schröder, M. High Capacity Hydrogen Adsorption in Cu(II) Tetracarboxylate Framework Materials: The Role of Pore Size, Ligand Functionalization, and Exposed Metal Sites. *J. Am. Chem. Soc.* **2009**, *131*, 2159–2171.

18 Yang, S.; Lin, X.; Dailly, A.; Blake, A. J.; Champness, N. R.; Hubberstey, P.; Schröder, M. Enhancement of H_2 Adsorption in Coordination Framework Materials by Use of Ligand Curvature. *Chem.—Eur. J.* **2009**, *15*, 4829–4835.

19 Wang, X.-S.; Ma, S.; Rauch, K.; Simmons, J. M.; Yuan, D.; Wang, X.; Yildirim, T.; Cole, W. C.; López, J. J.; de Meijere, A.; Zhou, H.-C. Metal–Organic Frameworks Based on Double-Bond-Coupled Di-Isophthalate Linkers with High Hydrogen and Methane Uptakes. *Chem. Mater.* **2008**, *20*, 3145–3152.

20 Zhao, D.; Yuan, D.; Yakovenko, A.; Zhou, H.-C. A NbO-type Metal–Organic Framework Derived from a Polyyne-coupled Di-isophthalate Linker formed in situ. *Chem. Commun.* **2010**, *46*, 4196–4198.

21 Yang, W.; Lin, X.; Jia, J.; Blake, A. J.; Wilson, C.; Hubberstey, P.; Champness, N. R.; Schröder, M. A Biporous Coordination Framework with High H_2 Storage Density. *Chem. Commun.* **2008**, 359–361.

22 Perry, J. J., IV; Perman, J. A.; Zaworotko, M. J. Design and Synthesis of Metal–Organic Frameworks Using Metal–Organic Polyhedra as Supermolecular Building Blocks. *Chem. Soc. Rev.* **2009**, *38*, 1400–1417.

23 Yan, Y.; Lin, X.; Yang, S.; Blake, A. J.; Dailly, A.; Champness, N. R.; Hubberstey, P.; Schröder, M. Exceptionally High H_2 Storage by a Metal–Organic Polyhedral Framework. *Chem. Commun.* **2009**, 1025–1027.

24 Yan, Y.; Telepeni, I.; Yang, S.; Lin, X.; Kockelmann, W.; Dailly, A.; Blake, A. J.; Lewis, W.; Walker, G. S.; Allan, D. R.; Barnett, S. A.; Champness, N. R.; Schröder, M. Metal-Organic Polyhedral Frameworks: High H_2 Adsorption Capacities and Neutron Powder Diffraction Studies. *J. Am. Chem. Soc.* **2010**, *132*, 4092–4094.

25 Yan, Y.; Blake, A. J.; Lewis, W.; Barnett, S. A.; Dailly, A.; Champness, N. R.; Schröder, M. Modifying Cage Structures in Metal–Organic Polyhedral Frameworks for H_2 Storage. *Chem.—Eur. J.* **2011**, *17*, 11162–11170.

26 Yan, Y.; Yang, S.; Blake, A. J.; Lewis, W.; Poirier, E.; Barnett, S. A.; Champness, N. R.; Schröder, M. A Mesoporous Metal–Organic Framework Constructed from a Nanosized C_3-Symmetric Linker and [Cu_{24}(isophthalate)$_{24}$] Cuboctahedra. *Chem. Commun.* **2011**, *47*, 9995–9997.

27 Yan, Y.; Suyetin, M.; Bichoutskaia, E.; Blake, A. J.; Allan, D. R.; Barnett, S. A.; Schröder, M. Modulating the Packing of [Cu_{24}(isophthalate)$_{24}$] Cuboctahedra in a Triazole-Containing Metal-Organic Polyhedral Framework. *Chem. Sci.* **2013**, *4*, 1731–1736.

28 Nouar, F.; Eubank, J. F.; Bousquet, T.; Wojtas, L.; Zaworotko, M. J.; Eddaoudi, M. Supermolecular Building Blocks (SBBs) for the Design and Synthesis of Highly Porous Metal—Organic Frameworks. *J. Am. Chem. Soc.* **2008**, *130*, 1833–1835.

29 Hong, S.; Oh, M.; Park, M.; Yoon, J. W.; Chang, J.-S.; Lah, M. S. Large H_2 Storage Capacity of a New Polyhedron-based Metal—Organic Framework with High Thermal and Hygroscopic Stability. *Chem. Commun.* **2009**, 5397–5399.

30 Zhao, D.; Yuan, D.; Sun, D.; Zhou, H.-C. Stabilization of Metal—Organic Frameworks with High Surface Areas by the Incorporation of Mesocavities with Microwindows. *J. Am. Chem. Soc.* **2009**, *131*, 9186–9188.

31 Yuan, D.; Zhao, D.; Sun, D.; Zhou, H.-C. An Isoreticular Series of Metal—Organic Frameworks with Dendritic Hexacarboxylate Ligands and Exceptionally High Gas-Uptake Capacity. *Angew. Chem., Int. Ed.* **2010**, *49*, 5357–5361.

32 Farha, O. K.; Yazaydin, A. Ö.; Eryazici, I.; Malliakas, C. D.; Hauser, B. G.; Kanatzidis, M. G.; Nguyen, S. T.; Snurr, R. Q.; Hupp, J. T. De Novo Synthesis of a Metal—Organic Framework Material Featuring Ultrahigh Surface Area and Gas Storage Capacities. *Nat. Chem.* **2010**, *2*, 944–948.

33 Farha, O. K.; Wilmer, C. E.; Eryazici, I.; Hauser, B. G.; Parilla, P. A.; O'Neill, K.; Sarjeant, A. A.; Nguyen, S. B. T.; Snurr, R. Q.; Hupp, J. T. Designing Higher Surface Area Metal—Organic Frameworks: Are Triple Bonds Better Than Phenyls? *J. Am. Chem. Soc.* **2012**, *134*, 9860–9863.

34 Farha, O. K.; Eryazici, I.; Jeong, N. C.; Hauser, B. G.; Wilmer, C. E.; Sarjeant, A. A.; Snurr, R. Q.; Nguyen, S. B. T.; Yazaydin, A. Ö.; Hupp, J. T. Metal—Organic Framework Materials with Ultrahigh Surface Areas: Is the Sky the Limit? *J. Am. Chem. Soc.* **2012**, *134*, 15016–15021.

35 Tan, C.; Yang, S.; Champness, N. R.; Lin, X.; Blake, A. J.; Lewis, W.; Schröder, M. High Capacity Gas Storage by a 4,8-Connected Metal—Organic Polyhedral Framework. *Chem. Commun.* **2011**, *47*, 4487–4489.

36 Ma, L.; Mihalcik, D. J.; Lin, W. Highly Porous and Robust 4,8-Connected Metal-Organic Frameworks for Hydrogen Storage. *J. Am. Chem. Soc.* **2009**, *131*, 4610–4612.

37 Peterson, V. K.; Liu, Y.; Brown, C. M.; Kepert, C. J. Neutron Powder Diffraction Study of D_2 Sorption in Cu_3(1,3,5-benzenetricarboxylate)$_2$. *J. Am. Chem. Soc.* **2006**, *128*, 15578–15579.